




High Strain Rate Ductility of the Selected Metals for Shaped Charge Liners [†]

Jacek Janiszewski ^{1,*} , Judyta Sienkiewicz ¹ , Wojciech Burian ², Aleksander Kowalski ², Artur Żak ³
and Paweł Prochenka ¹ 

¹ Faculty of Mechatronics, Armament and Aerospace, Military University of Technology, 00-908 Warsaw, Poland; judyta.sienkiewicz@wat.edu.pl (J.S.); pawel.prochenka@wat.edu.pl (P.P.)

² Institute of Non-Ferrous Metals, Łukasiewicz Research Network, 44-100 Gliwice, Poland; wojciech.burian@imn.lukasiewicz.gov.pl (W.B.); aleksander.kowalski@imn.lukasiewicz.gov.pl (A.K.)

³ Institute for Ferrous Metallurgy, Łukasiewicz Research Network, 44-100 Gliwice, Poland; artur.zak@imz.pl

* Correspondence: jacek.janiszewski@wat.edu.pl

[†] Presented at 19th International Conference on Experimental Mechanics, Kraków, Poland, 17–21 July 2022.

Abstract: An experimental study on various types of metals with the use of an electromagnetic expanding ring technique is presented in this paper. Three metals with differing physical–mechanical properties, i.e., OFE (oxygen-free electronic) copper, aluminum alloy AW 2017A, and Armco iron were considered. This study aimed to select a material with a desirable property for the performance of a shaped charged jet. The obtained results show that the OFE copper with the relatively smallest grain size reveals the highest ductility under electromagnetic expanding ring loading conditions. Armco iron rings also showed relatively good ductility under dynamic loading. These observations seem to suggest the possibility of applying the abovementioned metals in the manufacturing of shaped charge liners.

Keywords: shaped charge liner materials; high strain rate ductility; electromagnetic expanding ring test



Citation: Janiszewski, J.; Sienkiewicz, J.; Burian, W.; Kowalski, A.; Żak, A.; Prochenka, P. High Strain Rate Ductility of the Selected Metals for Shaped Charge Liners. *Phys. Sci. Forum* **2022**, *4*, 12. <https://doi.org/10.3390/psf2022004012>

Academic Editors: Zbigniew L. Kowalewski and Elżbieta Pieczyskasz

Published: 2 August 2022

Publisher's Note: MDPI stays neutral with regard to jurisdictional claims in published maps and institutional affiliations.



Copyright: © 2022 by the authors. Licensee MDPI, Basel, Switzerland. This article is an open access article distributed under the terms and conditions of the Creative Commons Attribution (CC BY) license (<https://creativecommons.org/licenses/by/4.0/>).

1. Introduction

The penetration capability of a shaped charged jet depends mainly on the density of material of shaped charge liner (SCL) ρ_j and the maximum length of the jet L . The theoretical possible penetration depth P can be estimated by applying the following equation:

$$P = L \sqrt{\frac{\rho_j}{\rho_t}} \quad (1)$$

whereby ρ_t denotes the target material density [1].

The maximum length of the unbroken jet is determined by two factors: jet velocity gradient, i.e., the velocity difference between jet tip v_{jmax} and cut-off velocity v_{jmin} , and break up time of jet t_f . In turn, both v_{jmax} and t_f are limited by other parameters. The maximum jet tip velocity v_{jmax} is limited by the bulk-sound velocity of the SCL material, whereas jet fragmentation time t_f depends directly on the ductile properties of the SCL material. In the literature of the field [1–3], it is emphasized that liner material ductility is critical to achieving a high-penetration capability of the jet. There are, however, two main problems associated with the issue of ensuring high ductility of the shaped charge jet, i.e., one connected with liner manufacturing technology and the second one associated with selection and/or a quality control procedure of ductile properties of the SCL material. The first problem is related to the transformation of the metallurgical state of the raw liner material into the desired metallurgical characteristics of the final SCL material. This problem is, however, not a straightforward procedure, because many different requirements have to

be met in order to guarantee the high ductility behavior of the SCL material. The most important of these requirements are: ensuring the homogeneity of the crystal structure in the entire volume of the liner material [4], ensuring a low content of impurities in the liner material ($<0.01\%$) [5,6], and obtaining a fine-grained structure of the liner material (average grain diameter from 10 to 50 μm) [7]. In turn, the second problem with the abovementioned results from many methodological and technical difficulties in testing the ductility of metals at high strain rates. Therefore, many investigators attempt to apply various experimental methods that allow for the assessing of the ductility of liner materials at high strain rates. The tensile split Hopkinson pressure bar technique is often applied to this purpose; however, it seems an expanding ring experiment is an excellent tool for examining the ductility behavior of metals [8,9].

The ring expansion test technique is based on a rapid radial acceleration of the thin-walled ring due to the detonation of an explosive charge or electromagnetic loading. As a result of such acceleration, in the first stage, the ring expands for a very short period (usually from several to several dozen microseconds) with a constantly increasing radial speed, and after reaching the maximum expansion speed, the ring wall decelerates due to internal circumferential stress of the ring material. By measuring the radial displacement $r(t)$ or velocity history $v(t)$ of the ring specimen for the deceleration phase of expansion (also called the inertial stage of expansion), the circumferential stress σ_θ and true strain ε_θ and strain rate for ring material can be determined [9].

In the present study, the electromagnetic expansion technique was used, originally applied by Gourdin [10], who suggested that the strain at fracture of ring specimens could be another liner material characteristic describing the ductility and fragmentation behavior of SCL materials. It was therefore decided to use the electromagnetic launch ring technique in performing experimental studies for three various materials, i.e., OFE copper, Al 2017A aluminum alloy, and Armco iron, to identify their ductility properties. The present study aims to evaluate and then select the material with desired plastic properties with regard to the high efficiency of shaped charge intended for the mining industry.

The paper is organized as follows: Section 2 is devoted to the characterization of the tested materials and the description of the experimental techniques applied to the determination of material ductility parameters. The results of the performed experimental tests on the ductility of the tested materials under electromagnetic expansion conditions and microscope investigations of fracture surfaces of ring fragments are described in Section 3, whereas the major conclusions of the present work are summarized in Section 4.

2. Materials and Methods

2.1. Materials

Three various materials with differing physical–mechanical properties were tested, i.e., the OFE copper manufactured by continuous extrusion forming (ConForm method), aluminum alloy AW 2017A, and Armco iron. Samples made of OFE copper exhibited a fully annealed microstructure (Figure 1a) that is typical for Cu after recrystallization. It is seen that a high number of annealing twins occurs in the structure. The grains of OFE copper were nearly equiaxed, and their average size was found to be about 40 μm , excluding twin boundaries.

Figure 1b represents an optical micrograph of the 2017A microstructure. It shows the grains of the solid solution α phase that are elongated in the rolling direction. Their average length and width are about 130 μm and 30 μm , respectively. Some precipitates such as Al–Cu and Al–Cu–Mg (identified by the EDS technique) are also observed in the material. As seen in Figure 1c, a sample made of Armco iron possesses a fully recrystallized microstructure with an average grain size of ~ 40 μm ; however, significant grain size deviations are observed, i.e., large (70 μm) and small (20 μm) grains are present.

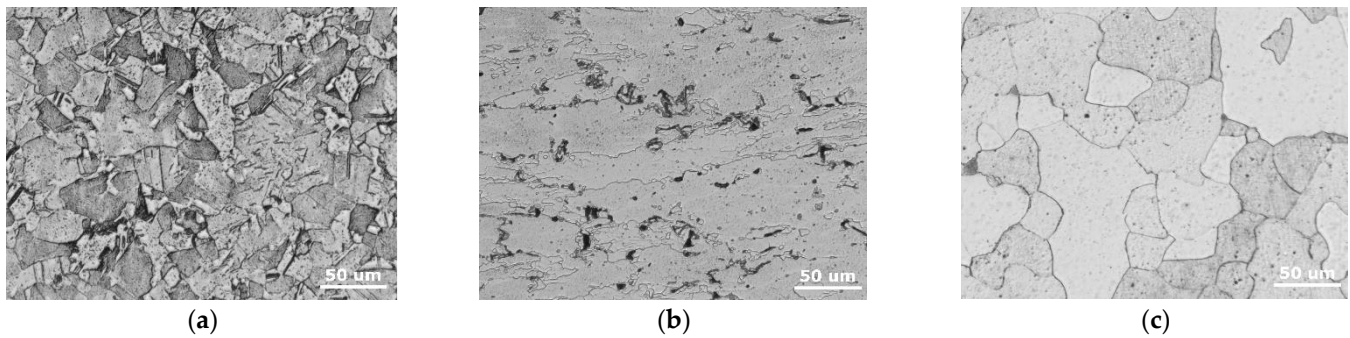


Figure 1. Microstructures of tested materials: (a) OFE copper (plane perpendicular to the extrusion direction); (b) Al 2017A; (c) Armco iron.

2.2. Experimental Procedures

The experimental investigation presented in the work was performed with the use of the electromagnetic expanding ring technique. A detailed description of the device (Figure 2a) applied in the present studies for an electromagnetic launch of the ring specimen is presented in [9,11]. The cross-sectional dimensions of the ring specimens for all tested materials were the same and equal to 1×1 mm; however, the inner diameter of the rings differed slightly, and they were as followed: for OFE copper and Al 2017A—31.2 mm, and for Armco iron—32.4 mm. This difference results from the use of slightly different methods of electromagnetic expansion of the ring specimens. The rings made of copper and aluminum alloy were expanded with the so-called direct method, i.e., the ring was slipped directly over the coil and then accelerated with electromagnetic forces (Figure 2b). In turn, the Armco iron rings, which are characterized by low conductivity, limiting the efficiency of electromagnetic launching, were first slipped over the so-called driver rings made of copper (high conductivity) and then accelerated through it (Figure 2c). The driver ring, also called the pusher, had the following dimensions: cross-section— 0.6×3 mm; inner diameter—31.2 mm. At least nine ring specimens for each test material were machined from the 50 mm diameter rod, except for OFE copper, which was taken from the 7 mm thick plate.

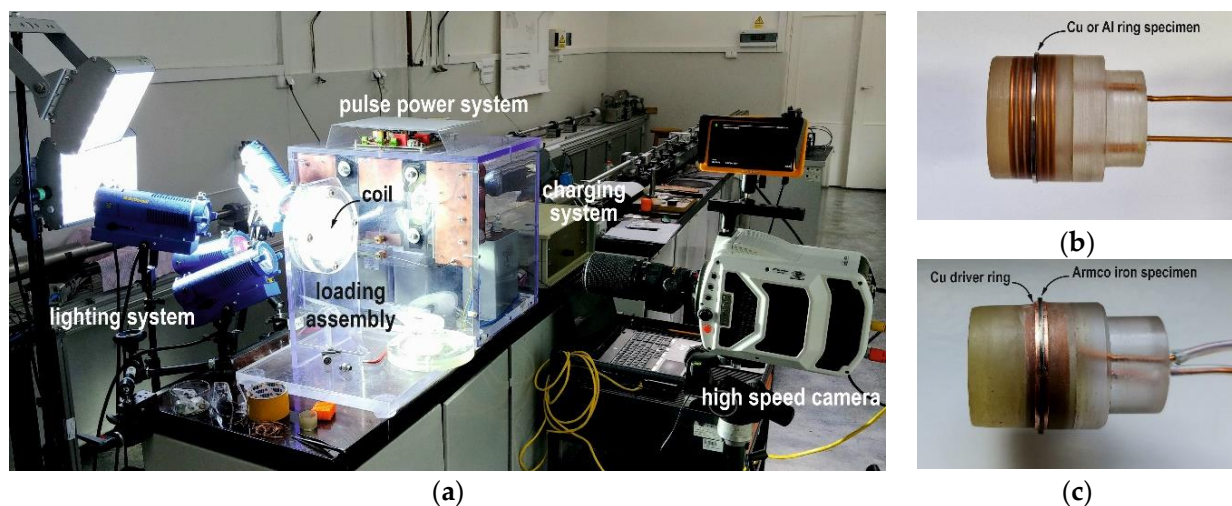


Figure 2. Electromagnetic ring expansion setup (a); solenoid coil used to direct expansion of the ring specimens made of OFE copper or aluminum (b); solenoid coil with the copper driver ring used for an indirect expansion of the Armco iron ring specimens (c).

The dynamic ductility of studied metals was expressed by uniform strain ϵ_u and strain at fracture ϵ_f . The parameter of ϵ_u was estimated by measuring changes in cross-

sectional areas in the uniform strain portions of the recovered ring fragments, whereas ε_f was calculated based on direct measurement of lengths of the recovered fragments captured into the soft medium (wax ring) [9]. Fragment length measurements were made using a Keyence VHX-6000 microscope (LM, KEYENCE Int., Mechelen, Belgium). In turn, the special measurement method presented in [12], as well as the Phantom v1612 digital high-speed camera (Vision Research, Inc., Wayne, NJ., USA) and specialized TEMA Automotive software (Image System AB, Linköping, Sweden) were used to determine rings expansion velocities.

In order to provide baseline material ductility, the quasistatic tensile tests for the selected metals were carried out with the use of small flat tensile specimens (gauge length—7 mm; gauge cross-section dimension— 2×2 mm). Material samples (three for each test material) were cut from the same raw materials as the ring specimens using wire electrical discharge machining technology.

The morphology of tested materials was studied using a light microscope (LM), scanning electron microscope (SEM), and energy-dispersive X-ray spectroscopy (EDS). Microstructural evaluation was carried out using a KEYENCE VHX-6000 digital microscope (LM, KEYENCE INTERNATIONAL, Mechelen, Belgium) and Phenom ProX/CeB₆ scanning electron microscope (SEM, Thermo Fisher Scientific, Eindhoven, The Netherlands) with an acceleration voltage 15 kV equipped with an energy dispersive spectroscopy (EDS) chemical composition analyzer. Grain size was evaluated by image analysis (Image J, National Institutes of Health, Bethesda, MD, USA) using at least 10 SEM cross-sectional images.

3. Results and Discussion

3.1. High Strain Rate Ductility

All expanding ring experiments were carried out under similar loading conditions, i.e., maximum expansion velocities were in a range from 135 m/s to 158 m/s, which corresponds to an average strain rate of the order of $8.1 \times 10^3 \text{ s}^{-1}$. Representative profiles of the expansion velocity curve for the tested metals are shown in Figure 3a. The highest maximum expansion velocities were reached for the rings made of OFE copper and Al 2017A, i.e., 158 and 157 m/s, respectively. On the other hand, the rings manufactured from Armco iron were expanded at the lowest velocities and equaled 135 m/s.

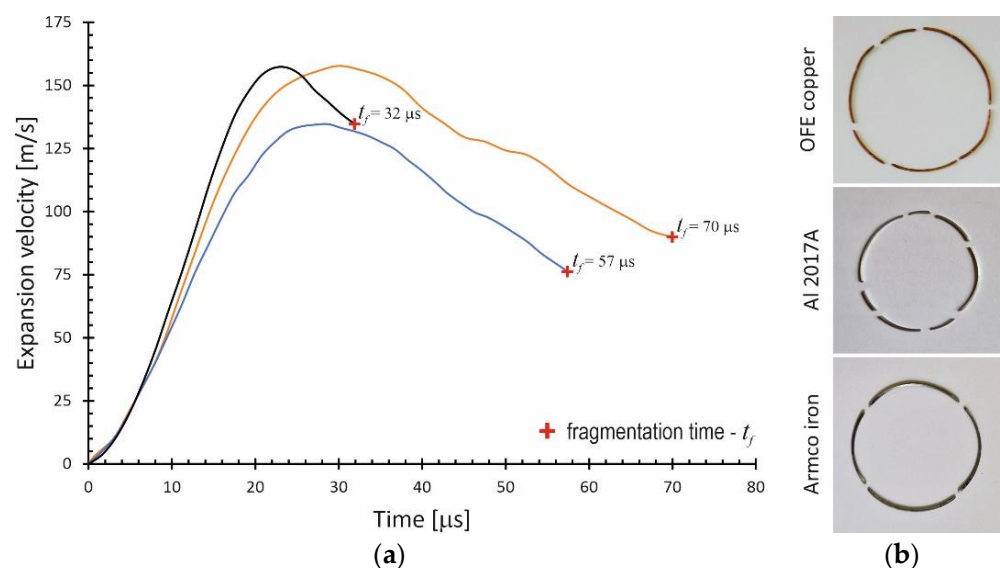


Figure 3. (a) Representative expansion velocity curves obtained from ring experiments performed for the OFE copper, 2017A aluminum alloy, and Armco iron; (b) view of recovered fragments generated from different sorts of material rings.

Depending on the type of tested material, the rings fragmented at different times (Figure 3a) and into a different number of fragments (Figure 3b). Fragmentation of OFE copper rings took place after the longest time, i.e., on average, after about $t_{fr} = 68 \pm 5 \mu s$, while Al 2017A rings fractured after the shortest time ($t_{fr} = 33 \pm 3 \mu s$) among all tested materials. On the other hand, the average fragmentation time for Armco iron rings was relatively long, and it was $t_{fr} = 54 \pm 6 \mu s$.

Rings made of Al 2017A were broken into the largest number of fragments (6 to 10 fragments), whereas the fewest fragments were observed for Armco iron rings (3 to 4 fragments). The number of fragments from OFE copper rings ranged from 5 to 7. The differences in the number of fragments result not only from the fragmentation susceptibility of the tested materials but also from the expansion velocity. Hence, the lowest number of fragments formed from Armco iron rings may also be a result of the relatively low expansion velocity.

The different fracture behavior of the tested materials under ring test conditions is also reflected in the values of the parameters determining their ductility. Values of strain at fracture— ϵ_f and uniform strain— ϵ_u , both for high strain rate and quasistatic experiments (uniform strain at quasi-static test— ϵ_{uq}), are collected in Table 1. These data allow one to conclude that the ductility of copper specimens is the highest ($\epsilon_f = 0.49$; $\epsilon_u = 0.41$) and increases by about 32% under an electromagnetic ring expansion experiment compared to the static one. In turn, the ductility of aluminum alloy of Al 2017A is the lowest ($\epsilon_f = 0.17$) of all tested SCL metals and, surprisingly, drops slightly under applied dynamic loading conditions (from $\epsilon_{uq} = 0.21$ to $\epsilon_u = 0.19$). Rings made of Armco iron revealed a relatively good ductility ($\epsilon_f = 0.25$). Interestingly, values of uniform strain obtained in the quasistatic and high strain rate tests are the same. Summarizing the above results, it can be stated that the OFE copper with the highest ductility under expansion ring test conditions should also show high ductile properties during the formation of the shaped charge jet.

Table 1. Ductility parameters for tested SCL materials determined under quasistatic and high strain rate testing conditions.

Ring Materials	Strain at Fracture ϵ_f (High Strain Rate) [-]	Uniform Strain ϵ_u (High Strain Rate) [-]	Uniform Strain ϵ_{uq} (Quasi-Static) [-]
OFE copper	0.49	0.41	0.31
Al 2017A	0.17	0.19	0.21
Armco iron	0.25	0.24	0.24

3.2. Microstructure and Fracture Analysis of Ring Fragments

A microstructure of the sample made of OFE copper after the electromagnetic ring test is shown in Figure 4a. The image was taken in the necking zone formed during the elongation and fracture of the ring specimen. Large plastic deformation—elongation—of the grains is visible in the deformed area. The voids that formed during the ring test are also present. As the material flows plastically, the cracks (voids) merge, leading to decohesion of the material. Figure 5a shows a fracture surface of the OFE copper fragment that exhibited a ductile nature with characteristic spherical docks and a surface with high roughness. In this type of fracture, slow crack propagation is accompanied by intense plastic deformation and the accumulation of deformation energy in the material.

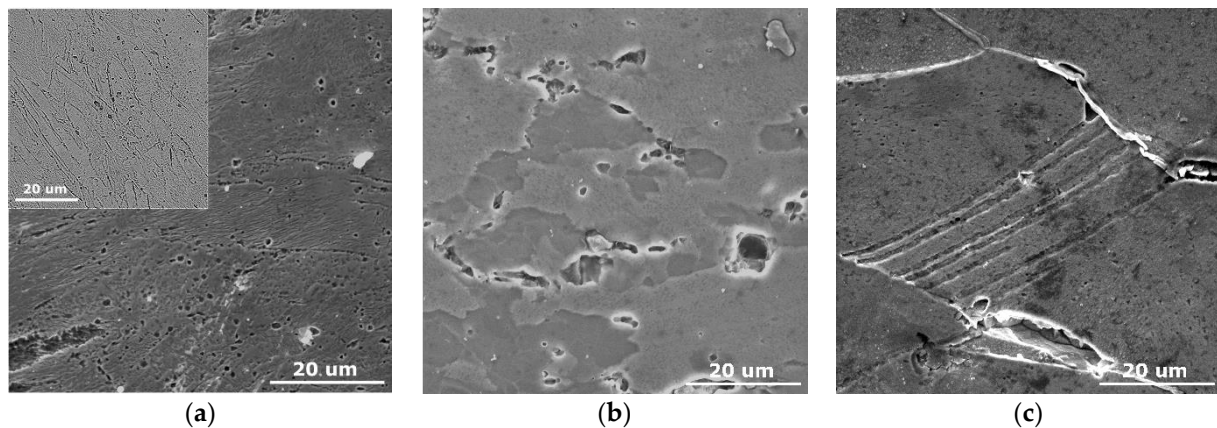


Figure 4. Microstructure in necking zones of ring fragments for (a) OFE copper, (b) 2017A aluminum alloy, (c) Armco iron.

The cross-sections of the sample made of 2017A aluminum alloy exhibit almost undistorted α phase grains relative to the initial structure (Figure 4b). Some decohesion has been noticed near the secondary phase. Detailed analysis of fracture surface for 2017A aluminum alloy (Figure 5b) showed that the microcracks were initiated on the precipitations. The secondary phase particles could cause stress concentration during the expansion, resulting in particles fragmentation, detachment, and initiation of microcracks.

Figures 4c and 5c represent the microstructure and fractures of the Armco iron fragments. There is a clear change in the shape of the grains in necking zones—the grains are flattened and elongated. The elongation of grains occurred in the direction parallel to the tensile stress tensor. Voids can also be seen across grain boundaries. In addition, twins, or so-called “Neumann lines”, can be seen in the grains. Neumann lines are groups of parallel lines that intersect at different angles. According to industrial alloy test results, Neumann lines can be considered to be traces of high pressures. The fractures formed on rings made of Armco iron show a ductile mode. Cracking of the material occurred along grain boundaries (intergranular cracking) because most of the particles on which voids were formed are located at grain boundaries. Fractographic investigations show that the formed ductile fractures are characterized by the presence of a developed fracture surface in the region of the specimen axis. The topography of this surface consists of numerous sets of holes (craters) of various sizes and shapes. The surface layer of the neck is dominated by the matrix shear mechanism and, therefore, the growth of microtubules and their subsequent merging occurs along the planes of maximum shear stresses. As a result, the parabolic shape of these discontinuities can be observed on the fracture surface, which is also visible in the fracture images.

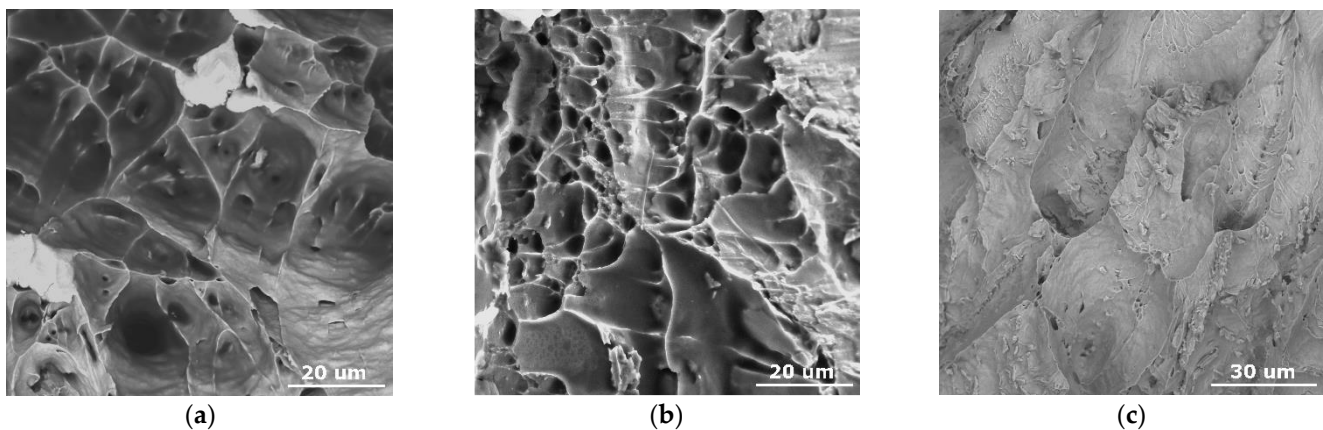


Figure 5. Fracture surface of ring fragments for (a) OFE copper, (b) 2017A aluminum alloy, (c) Armco iron.

4. Conclusions

Following the data presented in the literature [1–3], the obtained results show that the OFE copper with the highest ductility under an electromagnetic expanding ring experiment should meet requirements for SCL materials. This is also confirmed by microscopic studies of the crystal structure and topology of the surface fractures of the ring fragments. Microscopic analysis of OFE copper fragments revealed that fracture surfaces of necks formed in ring fragments clearly exhibit a ductile nature. Thus, it can be believed that applying the tested OFE copper as the liner material should ensure the high penetration capability of a shaped charge jet. Moreover, the obtained results for Armco iron reveal its good ductility properties under dynamic loading. It also suggests a possibility of applying the tested Armco iron in the manufacturing of shaped charge liners.

Author Contributions: Conceptualization, J.J. and J.S.; methodology, J.J. and J.S.; formal analysis, J.J.; investigation, J.J., J.S. and P.P.; resources, A.Ż., A.K. and W.B.; data curation, J.J. and J.S.; writing—original draft preparation, J.J. and J.S.; writing—review and editing, A.Ż., A.K. and W.B.; visualization, J.J., J.S. and P.P.; supervision, J.J.; project administration, W.B.; funding acquisition, W.B. All authors have read and agreed to the published version of the manuscript.

Funding: This research was funded by the Polish Ministry of Science and Higher Education, Centre for Research and Development under research grant No. TECHMATSTRATEG1/349156/13/NCBR/2017.

Institutional Review Board Statement: Not applicable.

Informed Consent Statement: Not applicable.

Data Availability Statement: Not applicable.

Conflicts of Interest: The authors declare no conflict of interest and the funders had no role in the design of the study; in the collection, analyses, or interpretation of data; in the writing of the manuscript; or in the decision to publish the results.

References

1. Walters, W.P.; Zukas, J.A. *Fundamentals of Shaped Charges*; John Wiley and Sons: New York, NY, USA, 1989.
2. Lichtenberger, A. Ductile behavior of some materials in the shaped charge jet. In *Metallurgical and Materials Applications of Shock-Wave and High-Strain-Rate Phenomena*; Murr, L.E., Staudhammer, K.P., Meyers, M.A., Eds.; Elsevier Science B.V.: Amsterdam, The Netherlands, 1995.
3. Lichtenberger, A. Some criteria for choice of shaped charge copper liners. In Proceedings of the 11th International Symposium on Ballistics, Brussels, Belgium, 9–11 May 1989.
4. Wiener, K.; Shaw, L.; Muelder, S.; Breithaupt, D.; Baum, D. Dynamic behavior of shear formed shaped charge liner. *Propellants Explos. Pyrotech.* **1993**, *18*, 345–351. [\[CrossRef\]](#)
5. Lassila, D.H. Correlations between shaped charge jet break up and grain boundary impurity concentrations. In Proceedings of the 13th International Symposium on Ballistics, Stockholm, Sweden, 1–3 June 1992.
6. Schwartz, A.J.; Lassila, D.H.; Baker, E.L. Analysis of intergranular impurity concentration and the effects on the ductility of copper shaped charge jets. In Proceedings of the 17th International Symposium on Ballistics, Midland, South Africa, 23–27 March 1998.
7. Bourne, B.; Jones, P.N.; Warren, R.H. Grain size and crystallographic texture effects on the performance of shaped charges. In Proceedings of the 14th International Symposium on Ballistics, Quebec, QC, Canada, 26–29 September 1993; pp. 119–124.
8. Zhang, H.; Ravi-Chandar, K. On the dynamics of necking and fragmentation—I. Realtime and post-mortem observations in Al 6061-O. *Int. J. Fract.* **2006**, *142*, 183–217. [\[CrossRef\]](#)
9. Janiszewski, J. Ductility of selected metals under electromagnetic ring test loading conditions. *Int. J. Solids Struct.* **2012**, *49*, 1001–1008. [\[CrossRef\]](#)
10. Gourdin, W.H. Analysis and assessment of electromagnetic ring expansion as a high-strain-rate test. *J. Appl. Phys.* **1989**, *65*, 411–422. [\[CrossRef\]](#)
11. Janiszewski, J.; Pichola, W. Development of electromagnetic ring expansion apparatus for high-strain-rate test. *Solid State Phenom.* **2009**, *147*, 645–650. [\[CrossRef\]](#)
12. Janiszewski, J. Measurement procedure of ring motion with the use of high-speed camera during electromagnetic expansion. *Metrol. Meas. Syst.* **2012**, *19*, 797–804. [\[CrossRef\]](#)